J|A|C|S
ARTICLES
Published on Web 08/27/2002

Divergent Pathways of C−H Bond Activation: Reactions of $(t\text{-}Bu_3PN)_2TiMe_2$ with Trimethylaluminum

James E. Kickham, Frédéric Guérin, and Douglas W. Stephan*

Contribution from the School of Physical Sciences, Chemistry and Biochemistry, University of Windsor, Windsor, Ontario, Canada N9B 3P4

Received March 5, 2002

Abstract: The reaction of $AlMe_3$ with $(t\text{-}Bu_3PN)_2TiMe_2$ **1** proceeds via competitive reactions of metathesis and C−H activation leading ultimately to two Ti complexes: $[(\mu^2\text{-}t\text{-}Bu_3PN)Ti(\mu\text{-}Me)(\mu^4\text{-}C)(AlMe_2)_2]_2$ **2**, $[(t\text{-}Bu_3PN)Ti(\mu^2\text{-}t\text{-}Bu_3PN)(\mu^3\text{-}CH_2)_2(AlMe_2)_2(AlMe_3)]$ **3**, and the byproduct $(Me_2Al)_2(\mu\text{-}CH_3)(\mu\text{-}NP(t\text{-}Bu_3))$ **4**. X-ray structural data for **2** and **3** are reported. Compound **3** undergoes thermolysis to generate a new species $[Ti(\mu^2\text{-}t\text{-}Bu_3PN)_2(\mu^3\text{-}CH_2)(\mu^3\text{-}CH)(AlMe_2)_3]$ **5**. Monitoring of the reaction of **1** with $AlMe_3$ by $^{31}P\{^1H\}$ NMR spectroscopy revealed intermediates including $(t\text{-}Bu_3PN)TiMe_3$ **6**. Compound **6** was shown to react with $AlMe_3$ to give **2** exclusively. Kinetic studies revealed that the sequence of reactions from **6** to **2** involves an initial C−H activation that is a second-order reaction, dependent on the concentration of Ti and Al. The second-order rate constant k_1 was $3.9(5) \times 10^{-4}$ M^{-1} s^{-1} ($\Delta H^{\neq} = 63(2)$ kJ/mol, $\Delta S^{\neq} = -80(6)$ J/mol·K). The rate constants for the subsequent C−H activations leading to **2** were determined to be $k_2 = 1.4(2) \times 10^{-3}$ s^{-1} and $k_3 = 7(1) \times 10^{-3}$ s^{-1}. Returning to the more complex reaction of **1**, the rate constant for the ligand metathesis affording **4** and **6** was $k_{met} = 6.1(5) \times 10^{-5}$ s^{-1} ($\Delta H^{\neq} = 37(3)$ kJ/mol, $\Delta S^{\neq} = -203(9)$ J/mol·K). The concurrent reaction of **1** leading to **3** was found to proceed with a rate constant of k_{obs} of $6(1) \times 10^{-5}$ s^{-1} ($\Delta H^{\neq} = 62(5)$ kJ/mol, $\Delta S^{\neq} = -118(17)$ J/mol·K). Using these kinetic data for these reactions, a stochastic kinetic model was used to compute the concentration profiles of the products and several intermediates with time for reactions using between 10 and 27 equivalents of $AlMe_3$. These models support the view that equilibrium between **1**·$AlMe_3$ and **1**·$(AlMe_3)_2$ accounts for varying product ratios with the concentration of $AlMe_3$. In a similar vein, similar equilibria account for the transient concentrations of **6** and an intermediate en route to **3**. The implications of these reactions and kinetic and thermodynamic data for both C−H bond activation and deactivation pathways for Ti-phosphinimide olefin polymerization catalysts are considered and discussed.

Introduction

Beginning with the landmark work from the groups of Graham[1] and Bergman[2] in the early 1980s, a variety of approaches to C−H activation have been examined.[3−5] Oxidative addition of alkanes to unsaturated d^8 and d^6 metals[6−12] and C−H additions to metal−ligand multiple bonds,[13] in particular d^0 metal imido systems,[14−26] are two strategies that have been extensively investigated. Sigma-bond metathesis of metal alkyls provides an alternative strategy that has also been exploited.[27−31]

* Address correspondence to this author. E-mail: Stephan@uwindsor.ca.

(1) Hoyano, J.; Graham, W. A. *J. Am. Chem. Soc.* **1982**, *104*, 3723.
(2) Janowicz, A. H.; Bergman, R. G. *J. Am. Chem. Soc.* **1983**, *105*, 3929−3939.
(3) Crabtree, R. H. *Chem. Rev.* **1995**, *95*, 987.
(4) Crabtree, R. H., Rapport, Z., Eds.; John Wiley & Sons: New York, 1992; p 653.
(5) Arndtsen, B. A.; Bergman, R. G.; Mobley, J. A.; Peterson, T. H. *Acc. Chem. Res.* **1995**, *28*, 154−162.
(6) Jones, W. D.; Hessell, E. T. *J. Am. Chem. Soc.* **1993**, *115*, 554−562.
(7) Burger, P.; Bergman, R. G. *J. Am. Chem. Soc.* **1993**, *115*, 10462.
(8) Arndtsen, B. A.; Bergman, R. G. *Science* **1995**, *270*, 1970−1973.
(9) Luecke, H. F.; Arndtsen, B. A.; Burger, P.; Bergman, R. G. *J. Am. Chem. Soc.* **1996**, *118*, 2517−2518.
(10) Holtcamp, M. W.; Labinger, J. A.; Bercaw, J. E. *J. Am. Chem. Soc.* **1997**, *119*, 848−849.
(11) Lin, M.; Sen, A. *Nature* **1994**, *368*, 613−614.
(12) Liuinstra, G. A.; Labinger, J. A.; Bercaw, J. E. *J. Am. Chem. Soc.* **1993**, *115*, 3004−3005.
(13) Howard, W. A.; Waters, M.; Parkin, G. *J. Am. Chem. Soc.* **1993**, *115*, 4917−4918.
(14) Schaller, C. P.; Cummins, C. C.; Wolczanski, P. T. *J. Am. Chem. Soc.* **1996**, *118*, 591−611.
(15) Cummins, C. C.; Schaller, C. P.; Van Duyne, G. D.; Wolczanski, P. T.; Chan, A. W. E.; Hoffmann, R. *J. Am. Chem. Soc.* **1991**, *113*, 2985−2994.
(16) Schaller, C. P.; Wolczanski, P. T. *Inorg. Chem.* **1993**, *32*, 131−144.
(17) Schaller, C. P.; Bananno, J. B.; Weoleczanski, P. T. *J. Am. Chem. Soc* **1994**, *116*, 4133−4134.
(18) De With, J.; Horton, A. D. *Angew. Chem., Int. Ed. Engl.* **1993**, *32*, 903−905.
(19) Walsh, P. J.; Hollander, F. J.; Bergmann, R. G. *Organometallics* **1993**, *12*, 3705−3723.
(20) Lee, S. Y.; Bergman, R. G. *j. Am. Chem. Soc.* **1995**, *117*, 5877−5878.
(21) Zambrano, C. H.; Profilet, R. D.; Hill, J. E.; Fanwick, P. E.; Rothwell, I. P. *Polyhedron* **1993**, *12*, 689−708.
(22) Jolly, M.; Mitchell, J. P.; Gibson, V. C. *J. Chem. Soc., Dalton Trans.* **1992**, 1329−1330.
(23) van der Heijden, H.; Hessen, B. T. *J. Chem. Soc., Chem. Commun.* **1995**, 145−146.
(24) Lockwood, M. A.; Clark, J. R.; Parkin, B. C.; Rothwell, I. P. *J. Chem. Soc., Chem. Commun.* **1996**, 1973−1974.
(25) Wigley, D. E. *Prog. Inorg. Chem.* **1994**, *42*, 239−482.
(26) Nugent, W. A.; Mayer, J. M. *Metal-Ligand Multiple Bonds*; Wiley-Interscience: New York, 1988.
(27) Guram, A. S.; Jordan, R. F.; Taylor, D. F. *J. Am. Chem. Soc.* **1991**, *113*, 1833−1835.
(28) Lecuyer, C.; Quiqnard, F.; Choplin, A.; Olivier, D.; Bassett, J. M. *Angew. Chem., Int. Ed. Engl.* **1991**, *30*, 1660−1661.

10.1021/ja0260972 CCC: $22.00

Most recently, Hartwig and co-workers applied this approach to effect catalytic hydroboration of alkanes, alkenes, and alkynes with a variety of metal catalysts.[32−37] This latter work exploits the combination of the reactivity of transition-metal species and the Lewis acidity of boron to promote B−C bond formation while generating reactive metal hydrides. Our interest in the interaction of Lewis acids with early transition-metal species began with the now conventional approach of using Lewis acids as activators for olefin polymerization catalysts.[38−43] In this area, we have developed and patented a new class of Ti-based catalysts containing phosphinimide ligands. This family of compounds of the form $Cp^{\dagger}Ti(NPR_3)X_2$ and $(R_3PN)_2TiX_2$ ($Cp^{\dagger}$ = Cp and analogues; R = alkyl, aryl; X = alkyl, halide) has proven to be highly active for ethylene polymerization catalysis under both laboratory and commercially relevant conditions.[44−48] Most notably, the species $(t\text{-}Bu_3PN)_2TiMe_2$ affords a remarkably active catalyst for the polymerization of ethylene upon activation with one equivalent of $[Ph_3C][B(C_6F_5)_4]$ or $B(C_6F_5)_3$.[48] Use of excess $B(C_6F_5)_3$, however, poisons catalytic activity by formation of the bis-zwitterion $(t\text{-}Bu_3PN)_2Ti(\mu\text{-}MeB(C_6F_5)_3)_2$.[49] Similarly, attempts to activate these phosphinimide-catalyst precursors with more conventional, commercial aluminum-based activators such as methylalumoxane (MAO) lead generally to significantly lower catalytic activity. Model studies of the interactions of several catalyst precursors with $AlMe_3$ (a component of most MAOs) revealed that C−H bond activation provides a reaction pathway for deactivation of these phosphinimide catalysts. In recent reports, we have described the quantitative triple C−H bond activation of $CpTi(NPR_3)Me_2$ yielding $TiAl_3$- and $TiAl_4$-carbide species.[50,51] The analogous chemistry with Zr-phosphinimide complexes yields Zr-methanide species $(Cp^*Zr)_4(\mu\text{-}Cl)_5(Cl)(\mu\text{-}CH)_2$ and $(Cp^*Zr)_5(\mu\text{-}Cl)_6(\mu\text{-}CH)_3$ with concurrent ligand abstraction.[52]

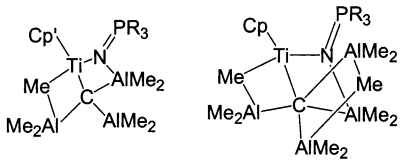

In this paper, we examine the reactions of $(t\text{-}Bu_3PN)_2TiMe_2$ **1** with $AlMe_3$ in detail. Synthetic, structural, and kinetic work reveal that phosphinimide ligand metathesis followed by sequential C−H bond activation affording a $TiAl_2$ carbide dimer is competitive with direct C−H activation of **1**. The details of these divergent pathways of C−H activation are examined. The implications of these findings for both olefin polymerization catalysis and C−H bond activation are considered.

Experimental Section

General Data. All preparations were done under an atmosphere of dry, O_2-free N_2 employing both Schlenk line techniques and Innovative Technologies, Mbraun, or Vacuum Atmospheres inert atmosphere gloveboxes. Solvents were purified employing Grubbs' type column systems manufactured by Innovative Technology. All organic reagents were purified by conventional methods. ^1H and $^{13}C\{^1H\}$ NMR spectra were recorded on Bruker Avance-300 and 500 NMR spectrometers operating at 300.13 and 500.13 MHz, respectively. Trace amounts of protonated solvents were used as ^1H NMR reference and chemical shifts are reported in ppm relative to $SiMe_4$. $^{31}P\{^1H\}$ NMR spectra were recorded on a Bruker Avance-300 spectrometer and referenced to 85% H_3PO_4. All NMR spectra were recorded at 25 °C in C_6D_6 unless otherwise indicated. The corresponding thermodynamic parameters were determined using the appropriate mathematical relationships. Guelph Chemical Laboratories Inc. of Guelph, Ontario performed combustion analyses. Preparation of complexes of the form $(t\text{-}Bu_3PN)_2TiMe_2$ **1** and $(t\text{-}Bu_3PN)TiMe_3$ **6** were performed as previously described in the literature.[53] In a similar manner, the species $(t\text{-}Bu_3PN)_2Ti(^{13}Me)_2$ ^{13}**1** was prepared employing $^{13}MeMgBr$. $AlMe_3$ was purchased from the Aldrich Chemical Co.

Synthesis of $[(\mu^2\text{-}t\text{-}Bu_3PN)Ti(\mu^4\text{-}C)(AlMe_2)(AlMe_2(\mu\text{-}Me))]_2$ 2 and $[(t\text{-}Bu_3PN)Ti(\mu^2\text{-}t\text{-}Bu_3PN)(\mu^3\text{-}CH_2)_2(AlMe_2)_2(AlMe_3)]$ 3. Compound **1** (0.301 g, 0.587 mmol) was dissolved in benzene (5 mL) and $AlMe_3$ (1.5 mL, 2.0 M in hexanes, 3.0 mmol) was added via syringe. The solution was stirred overnight in a scintered glass vial during which time the solution developed a red color with a blood-red precipitate. The suspension was then allowed to stand for two days. The orange solution was decanted and the blood-red solid **2** was washed with hexanes (2 × 4 mL) and dried in vacuo. Yield: 0.110 g (46%). Recrystallization of **2** from CH_2Cl_2 or C_6H_6 gave X-ray quality crystals. To the decanted orange solution was added hexanes (5 mL). After about 2 h, the hexanes/benzene solution was decanted from a peach-colored solid **3**, which was then dried in vacuo. Yield 0.111 (27%). Recrystallization of **3** from C_6H_6/hexanes gave X-ray quality crystals. Compound ^{13}**2** was similarly isolated employing labeled $(t\text{-}Bu_3PN)_2Ti(^{13}Me)_2$ ^{13}**1**. **2**: ^1H NMR (CD_2Cl_2): 1.40 (d, $^3J_{PH}$ = 14 Hz, 54H, PC(CH_3)$_3$); 1.21 (s, 6H, Ti−CH_3); −0.08 (s, 6H, Al−CH_3); −0.54 (s, 6H, Al−CH_3); −1.16 (s, 6H, Al−CH_3); −1.29 (s, 6H, Al−CH_3). $^{31}P\{^1H\}$ NMR (CD_2Cl_2): 68.2 (s, *P*C(CH_3)$_3$). $^{13}C\{APT\}$ NMR (CD_2Cl_2): 463.0 (s, *C*(Ti_2Al_2)); 40.4 (d, $^1J_{PC}$ = 46 Hz, P*C*(CH_3)$_3$); 30.8 (s, PC(*C*H$_3$)$_3$); 26.9 (s, Ti−*C*H$_3$); −1.6 (br-s, Al−*C*H$_3$); −3.0 (br-s, Al−*C*H$_3$); −4.7 (br-s, Al−*C*H$_3$); −7.1 (br-s, Al−*C*H$_3$). EA (Calcd for $C_{36}H_{84}Al_4N_2P_2Ti_2$): C, 53.33; H, 10.44; N, 3.46; Found: C, 53.27; H, 10.31; N, 3.27. **3**: ^1H NMR: 5.33 (d, ^2J = 12 Hz, 1H, CH_2-a); 5.06 (d, ^2J = 12 Hz,

(29) Thompson, M. E.; Baxter, S. M.; Bulls, A. R.; Burger, B. J.; Nolan, M. C.; Santarsiero, B. D.; Schaefer, W. P.; Bercaw, J. E. *J. Am. Chem. Soc.* **1987**, *109*, 203−219.
(30) Watson, P. I.; Parshall, G. W. *Acc. Chem. Res.* **1985**, *18*.
(31) Fendrick, C. M.; Marks, T. K. *J. Am. Chem. Soc.* **1986**, *108*, 425−437.
(32) Waltz, K. M.; He, X.; Muhoro, C.; Hartwig, J. F. *J. Am. Chem. Soc.* **1995**, *117*, 11357−11358.
(33) Muhoro, C. N.; He, X.; Hartwig, J. F. *J. Am. Chem. Soc.* **1999**, *121*, 5033−5046.
(34) Waltz, K. M.; Muhoro, C. N.; Hartwig, J. F. *Organometallics* **1999**, *18*, 3383−3393.
(35) Waltz, K. M. l.; Hartwig, J. F. *Science* **1997**, *277*, 211−213.
(36) Muhoro, C. N.; Hartwig, J. F. *Angew. Chem., Int. Ed. Engl.* **1997**, *36*, 1510−1512.
(37) He, X.; Hartwig, J. F. *J. Am. Chem. Soc.* **1996**, *118*, 1696−1702.
(38) Hlatky, G. G. *Coord. Chem. Rev.* **2000**, *199*, 235−329.
(39) Weckhuysen, B. M.; Schoonheydt, R. A. *Catal. Today* **1999**, *51*, 215−221.
(40) Yasuda, H.; Ihara, E. *Bull. Chem. Soc. Jpn.* **1997**, *70*, 1745−1767.
(41) Theopold, K. H. *Eur. J. Inorg. Chem.* **1998**, 15−24.
(42) Hlatky, G. G. *Coord. Chem. Rev.* **1999**, *181*, 243−296.
(43) Kaminsky, W. *J. Chem. Soc., Dalton Trans.* **1998**, 1413−1418.
(44) Brown, S. J.; Gao, X.; Harrison, D. G.; McKay, I.; Koch, L.; Wang, Q.; Xu, W.; Von Haken Spence, R. E.; Stephan, D. W. In *PCT Int. Appl.*; Nova Chemicals Corporation: Can., WO, 2000; p 33.
(45) Stephan, D. W.; Stewart, J. C.; Brown, S. J.; Swabey, J. W.; Wang, Q. In *Eur. Pat. Appl.*; Switz, S. A., Ed.; Nova Chemicals (International): EP, 1998; p 17.
(46) Stephan, D. W.; Stewart, J. C.; Harrison, D. G. In *Eur. Pat. Appl.*; Switz, S. A., Ed.; Nova Chemicals (International): EP, 1999; pp 21.
(47) Stephan, D. W.; Stewart, J. C.; Guerin, F.; Spence, R. E. v. H.; Xu, W.; Harrison, D. G. *Organometallics* **1999**, *18*, 1116−1118.
(48) Stephan, D. W.; Guerin, F.; Spence, R. E. v. H.; Koch, L.; Gao, X.; Brown, S. J.; Swabey, J. W.; Wang, Q.; Xu, W.; Zoricak, P.; Harrison, D. G. *Organometallics* **1999**, *18*, 2046−2048.
(49) Guerin, F.; Stephan, D. W. *Angew. Chem., Int. Ed.* **2000**, *39*, 1298−1300.
(50) Kickham, J. E.; Guerin, F.; Stewart, J. C.; Stephan, D. W. *Angew. Chem., Int. Ed.* **2000**, *39*, 3263−3266.
(51) Kickham, J. E.; Guerin, F.; Stewart, J. C.; Urbanska, E.; Ong, C. M.; Stephan, D. W. *Organometallics* **2001**, *20*, 3209.
(52) Yue, N.; Hollink, E.; Guérin, F.; Stephan, D. W. *Organometallics* **2001**, *20*, 4424−4433.
(53) Guerin, F.; Stewart, J. C.; Beddie, C.; Stephan, D. W. *Organometallics* **2000**, *19*, 2994−3000.

1H, CH_2-a); 3.84 (br-s, 1H, CH_2-b); 1.80 (br-s, 1H, CH_2-b); 1.24 (d, $^3J_{PH}$ = 13 Hz, 27H, PC(CH_3)$_3$); 1.17 (d, $^3J_{PH}$ = 13 Hz, 27H, PC(CH_3)$_3$); 0.17 (s, 3H, AlCH_3); 0.02 (s, 3H, AlCH_3); −0.11 (s, 3H, AlCH_3); −0.14 (s, 9H, Al(CH_3)$_3$); −0.41 (s, 3H, AlCH_3). ^{31}P{^{1}H} NMR: 69.0 (s, TiN-(Al)*P*C(CH$_3$)$_3$); 40.9 (s, TiN*P*C(CH$_3$)$_3$). ^{13}C{APT} NMR: 113.3 (br-s, *C*H$_2$-a); 88.6 (br-s, CH_2-b); 41.8 (d, $^2J_{PC}$ = 45 Hz, P*C*(CH$_3$)$_3$); 40.6 (d, $^1J_{PC}$ = 45 Hz, P*C*(CH$_3$)$_3$); 30.4 (s, PC(*C*H$_3$)$_3$), 30.0 (s, PC(*C*H$_3$)$_3$); −0.1, −1.4, −3.4, −5.2, −6.4 (s, AlMe$_x$). EA (Calcd for $C_{36}H_{84}Al_4N_2P_2Ti_2$): C, 53.33; H, 10.44; N, 3.46; Found: C, 53.27; H, 10.31; N, 3.27.

Alternative Synthesis of 2. Compound **6** (0.280 g, 0.905 mmol) was dissolved in hexanes (10 mL) and $AlMe_3$ (0.44 mL, 2.0 M in hexanes, 4.6 mmol) was added via syringe. The solution was stirred overnight in a scintered glass vial during which time the solution developed a pale-red color with a blood-red precipitate. The hexanes were decanted from the solid, which was washed with hexanes (3 × 5 mL) and dried in vacuo. Yield: 0.314 g (86%). The NMR spectra of this compound were identical with those of carbide **2**.

Generation of (Me$_2$Al)$_2$(μ-CH$_3$)(μ-NP(*t*-Bu$_3$)) 4. *t*-Bu$_3$PNH (0.027 g, 0.124 mmol) was added to a resealable NMR tube and then dissolved in benzene-d_6 (~0.5 mL). $AlMe_3$ (0.124 mL, 2.0 M in hexanes, 0.248 mmol) was added to the NMR tube which was immediately sealed and heated at 60 °C for 16 h. ^{1}H NMR (C_6D_6, δ ppm): 1.13 (d, $^3J_{PH}$ = 13 Hz, 27H, PC(CH_3)$_3$); 0.56 (br-s, 3H, Al(μ-CH_3)Al); −0.23 (br-s, 12H, AlCH_3). ^{31}P{^{1}H} NMR: 61.0. ^{13}C{^{1}H} NMR: 40.2 (d, $^1J_{PC}$ = 48 Hz, P*C*(CH$_3$)$_3$); 30.3 (s, PC(*C*H$_3$)$_3$); unobserved (AlMe$_x$). The extreme sensitivity and pyrophoric nature of this compound precluded elemental analysis. NMR spectra of this species are included in the supplementary data.

Generation of [(*t*-Bu$_3$PN)Ti(μ^2-*t*-Bu$_3$PN)(μ^3-CH$_2$)(μ^3-CH)(AlMe$_2$)$_3$] 5. Compound **3** (0.010 g) was added to a resealable NMR tube and then dissolved in C_6D_6 (0.50 mL). The solution was heated at 60 °C for 26 h. ^{1}H NMR: 5.87 (s, 1H, (Me$_2$Al)C*H*(Ti)(AlMe$_2$)); 3.00 (d, $^2J_{HH}$ = 8 Hz, 1H, (Me$_2$Al)CH_2Ti(AlMe$_2$); 1.37 (d, $^2J_{HH}$ = 8 Hz, 1H, (Me$_2$-Al)CH_2(Ti)(AlMe$_2$); 1.30 (d, $^3J_{PH}$ = 13 Hz, 27H, PC(CH_3)$_3$); 1.22 (d, $^3J_{PH}$ = 13 Hz, 27H, PC(CH_3)$_3$); 0.11 (s, 3H, AlCH_3); 0.04 (s, 9H, AlCH_3); −0.21 (s, 3H, AlCH_3); −0.37 (s, 3H, AlCH_3). ^{31}P{^{1}H} NMR: 63.2 (s); 65.5 (s). ^{13}C{APT} NMR: 227.2 (s, (Me$_2$Al)-*C*H(Ti)(AlMe$_2$)); 68.9 (s, (Me$_2$Al)CH_2(Ti)(AlMe$_2$)); 41.2 (d, $^1J_{PC}$ = 45.2 Hz, P*C*(CH$_3$)$_3$); 40.7 (d, $^1J_{PC}$ = 45.2 Hz, P*C*(CH$_3$)$_3$); 30.8 (s, PC(*C*H$_3$)$_3$); 30.7 (s, PC-(*C*H$_3$)$_3$). The inability to generate **5** cleanly or to separate it from **3** precluded elemental analysis. NMR spectra of this species are included in the supplementary data.

Kinetic Studies. In a typical kinetic experiment, **1** (0.021 g, 41 μmol) or **6** (0.020 g, 65 μmol) was weighed in an inert atmosphere drybox into a resealable NMR tube equipped with a Teflon screw cap. The appropriate amounts of C_6D_6 and $AlMe_3$ were then measured into the NMR tube to give [**1**]$_0$ or [**6**]$_0$ of approximately 0.075 mol L^{-1}. The NMR tube was sealed and shaken to ensure proper mixing, resulting in an initially pale-beige solution. Typical kinetic experiments were performed at 298 K, while thermodynamic data were obtained via variable temperature experiments by placing the NMR tube in the spectrometer, which had been previously adjusted to the required temperature. Thirty-two ^{31}P{^{1}H} NMR spectra were recorded at 30 min intervals over 16 h with individual spectra requiring 8:13 min for acquisition followed by a delay of 21:47 min. A delay of 15 s was used between 32 consecutive 30°-pulses to ensure full relaxation of all phosphorus species. The time of individual spectra was noted upon completion of the 32nd pulse.

X-ray Data Collection and Reduction. X-ray quality crystals of **2** and **3** were obtained directly from the preparation as described above. The crystals were manipulated and mounted in capillaries in a glovebox, thus maintaining a dry, O_2-free environment for each crystal. Diffraction experiments were performed on a Siemens SMART System CCD diffractometer collecting a hemisphere of data in 1329 frames with 10-s exposure times. Crystal data are summarized in Table 1. The observed extinctions were consistent with the space groups in each case. The data sets were collected (4.5° < 2θ < 45−50.0°). The data were processed using the SAINT and XPREP processing package, and an empirical absorption correction based on redundant data was applied. Subsequent solution and refinement was performed using the SHELXTL solution package.

Table 1. Crystallographic Parameters[a]

	2	**3**
formula	$C_{36}H_{84}Al_4N_2P_2Ti_2$	$C_{33}H_{79}Al_3N_2P_2Ti$
formula weight	810.72	694.76
a (Å)	12.82150(10)	12.5077(14)
b (Å)	18.71910(10)	16.875(2)
c (Å)	19.8293(4)	20.575(2)
β (deg)		94.063(2)
cryst syst	orthorhombic	monoclinic
space group	$P2_12_12_1$	$P2_1/n$
vol (Å^3)	4759.17(11)	4331.7(9)
D_{calcd}(gcm^{-1})	1.131	1.065
Z	4	4
abs coeff, μ, mm^{-1}	0.501	0.354
data collected	24014	18815
data $F_o^2 > 3\sigma(F_o^2)$	8297	6219
variables	433	386
R (%)	6.29	0.0561
R_w (%)	14.58	0.1147
goodness of fit	0.964	0.798

[a] All data collected at 24 °C with Mo Kα radiation (λ = 0.71069 Å), $R = \Sigma||F_o| - |F_c||/\Sigma|F_o|$, $R_w = [\Sigma[\omega(F_o^2 - F_c^2)^2]/\Sigma[\omega F_o^2)^2]]^{0.5}$.

Structure Solution and Refinement. Non-hydrogen atomic scattering factors were taken from the literature tabulations.[54] The heavy atom positions were determined using direct methods employing either of the SHELXTL direct methods routines. The remaining non-hydrogen atoms were located from successive difference Fourier map calculations. The refinements were carried out by using full-matrix least-squares techniques on *F*, minimizing the function $\omega(|F_o| - |F_c|)^2$ where the weight ω is defined as $4F_o^2/2\sigma(F_o^2)$ and F_o and F_c are the observed and calculated structure factor amplitudes. In the final cycles of each refinement, all non-hydrogen atoms were assigned anisotropic temperature factors. Carbon-bound hydrogen atom positions were calculated and allowed to ride on the carbon to which they are bonded assuming a C−H bond length of 0.95 Å. Hydrogen atom temperature factors were fixed at 1.10 times the isotropic temperature factor of the carbon atom to which they are bonded. The hydrogen atom contributions were calculated but not refined. The final values of refinement parameters are given in Table 1. The locations of the largest peaks in the final difference Fourier map calculation as well as the magnitude of the residual electron densities in each case were of no chemical significance. Positional parameters, hydrogen atom parameters, thermal parameters, and bond distances and angles have been deposited as Supporting Information.

Results and Discussion

The reaction of $AlMe_3$ with (*t*-Bu$_3$PN)$_2$TiMe$_2$ **1** at room temperature in benzene proceeds with elimination of methane gas and the subsequent precipitation of a blood-red product **2** in 46% yield. ^{1}H NMR data for **2** in CD_2Cl_2 revealed the presence of five different methyl environments with integral intensity ratios of 1:1:1:1:1. One phosphinimide ligand environment was evident from the ^{1}H data, and the corresponding ^{31}P-{^{1}H} NMR spectrum showed a singlet resonance at 68.2 ppm. ^{13}C{^{1}H} NMR data were less informative, containing resonances for only the *tert*-butyl groups of the phosphinimide ligand at 30.8 and 40.5 ppm. Additional data were obtained from the corresponding reaction of the ^{13}C labeled (*t*-Bu$_3$PN)$_2$Ti^{13}Me$_2$

(54) Cromer, D. T.; Mann, J. B. *Acta Crystallogr., Sect. A* **1968**, *A24*, 321−324.

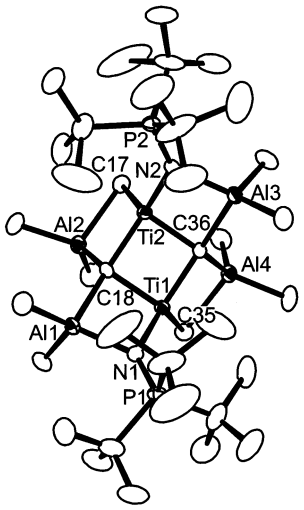

Figure 1. ORTEP drawings of **2**, 20% thermal ellipsoids are shown. Hydrogen atoms have been omitted for clarity. Ti(1)−C(18) 1.918(6); Ti(1)−C(36) 1.949(5); Ti(1)−N(1) 2.015(5); Ti(1)−C(35) 2.237(7); Ti(1)−Al(1) 2.726(2); Ti(1)−Ti(2) 2.7583(14); Ti(1)−Al(4) 2.774(2); Ti(2)−C(36) 1.914(5); Ti(2)−C(18) 1.968(5); Ti(2)−N(2) 2.027(4); Ti(2)−C(17) 2.223(7); Al(1)−N(1) 1.971(5); Al(1)−C(18) 2.052(5); Al(2)−C(18) 2.024(6); Al(3)−N(2) 1.980(5); Al(3)−C(36) 2.063(6); Al(4)−C(36) 2.027(6); P(1)−N(1) 1.602(5); P(2)−N(2) 1.592(5); C(18)−Ti(1)−C(36) 89.4(2); C(18)−Ti(1)−N(1) 92.5(2); C(36)−Ti(1)−N(1) 136.3(2) C(18)−Ti(1)−C(35) 115.7(3); C(36)−Ti(1)−C(35) 97.3(3); N(1)−Ti(1)−C(35) 120.6(2); C(36)−Ti(2)−C(18) 88.9(2); C(36)−Ti(2)−N(2) 92.8(2); C(18)−Ti(2)−N(2) 137.2(2); C(36)−Ti(2)−C(17) 117.3(3); C(18)−Ti(2)−C(17) 97.3(3); N(2)−Ti(2)−C(17) 119.3(3); N(1)−Al(1)−C(18) 89.8(2); C(18)−Al(2)−C(17) 96.4(2); N(2)−Al(3)−C(36) 89.8(2); C(36)−Al(4)−C(35) 96.0(3); P(1)−N(1)−Al(1) 137.6(3); P(1)−N(1)−Ti(1) 135.9(3); Al(1)−N(1)−Ti(1) 86.3(2); P(2)−N(2)−Al(3) 138.0(3); P(2)−N(2)−Ti(2) 135.8(3); Al(3)−N(2)−Ti(2) 86.05(18); Al(2)−C(17)−Ti(2) 77.8(3); Ti(1)−C(18)−Ti(2) 90.4(2); Ti(1)−C(18)−Al(2) 125.6(3); Ti(2)−C(18)−Al(2) 88.1(2); Ti(1)−C(18)−Al(1) 86.7(2); Ti(2)−C(18)−Al(1) 149.4(3); Al(2)−C(18)−Al(1) 118.0(3); Al(4)−C(35)−Ti(1) 77.3(2); Ti(2)−C(36)−Ti(1) 91.1(2); Ti(2)−C(36)−Al(4) 126.5(3); Ti(1)−C(36)−Al(4) 88.5(2); Ti(2)−C(36)−Al(3) 86.8(2); Ti(1)−C(36)−Al(3) 150.1(3); Al(4)−C(36)−Al(3) 116.5(3).

^{13}**1** which was prepared using $^{13}CH_3MgBr$. The ^{1}H NMR spectrum of ^{13}**2** is similar to that of **2** with the notable addition of ^{13}C satellites ($^1J_{CH} \sim 112$ Hz) flanking the $AlMe_2$ resonances. While a $^{13}C\{^1H\}$ NMR resonance at 26.9 ppm was assigned to a Ti bound methyl group, resonances at −1.6, −3.0, −4.7, and −7.1 ppm were assigned to Al bound methyl groups. Most notably, a resonance appears at 463.0 ppm. This compares with resonances observed for $[Co_6C(CO)_{13}\{AuPPh_3\}]^-$,[55] $[Fe_5MoAuC(CO)_{17}(L)]^-$,[56] and $[Fe_5C(CO)_{14}\{HgM\}]^-$[57] suggesting the presence of a carbide carbon.

Recrystallization of **2** from benzene afforded X-ray quality crystals permitting the unambiguous formulation as a $Ti_2Al_4C_2$ cluster of formulation $[(\mu^2\text{-}t\text{-}Bu_3PN)Ti(\mu\text{-}Me)(\mu^4\text{-}C)(AlMe_2)_2]_2$ (Figure 1). This species is comprised of two intersecting sets of ladders each composed of three four-membered rings. The central four-membered ring, common to both ladders, is a Ti_2C_2 core, in which two carbide atoms bridge the two Ti centers. Two phosphinimide ligands and the two carbides bridge each of the titanium atoms to two $AlMe_2$ centers. Thus, the central Ti_2C_2 ring and two TiN_2Al rings form the one ladder of three four-membered rings. The carbide carbons also bridge to another $AlMe_2$ center. One of the methyl groups on each of these Al atoms bridges to Ti completing the second ladder of three contiguous four-membered rings. Overall, the molecule resembles a "saddle" shaped geometry, with the two phosphinimide ligands on one side of the saddle and the four $AlMe_2$ fragments on the other. The geometries about the Ti and C atoms of the central Ti_2C_2 core of **2** are significantly distorted from tetrahedral (Figure 3a). Angles at Ti within the four-membered rings range from 88.9(2)−97.3(3)°, whereas the remaining angles at Ti lie between 115.7(3)−137.2(2)°. Similarly, the angles about the carbides range between 86.8(2)−90.4(2)° for those inside four-membered rings and as high as 150.1(3)° for those between rings. The steric demands of the phosphinimide ligands as well as the geometric constraints imposed by fused four-membered rings presumably account for these distorted

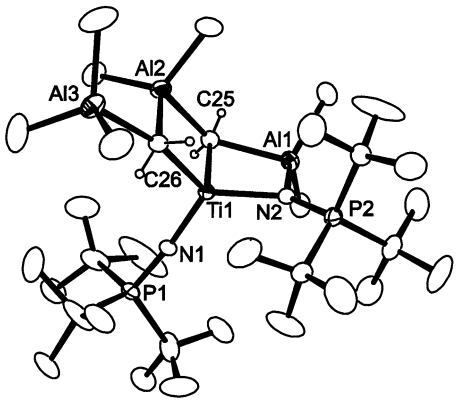

Figure 2. ORTEP drawings of **3**, 20% thermal ellipsoids are shown. Hydrogen atoms have been omitted for clarity. Ti(1)−N(1) 1.793(4); Ti(1)−N(2) 1.991(4); Ti(1)−C(25) 2.013(7); Ti(1)−C(26) 2.125(6); Al(1)−N(2) 1.962(4); Al(1)−C(25) 2.136(6); Al(2)−C(26) 2.003(6); Al(2)−C(25) 2.220(7); Al(3)−C(26) 2.196(6); P(1)−N(1) 1.597(4); P(2)−N(2) 1.609(4); N(1)−Ti(1)−N(2) 121.48(16); N(1)−Ti(1)−C(25) 108.4(3); N(2)−Ti(1)−C(25) 94.4(2); N(1)−Ti(1)−C(26) 109.4(2); N(2)−Ti(1)−C(26) 120.1(2); C(25)−Ti(1)−C(26) 97.7(2); N(2)−Al(1)−C(25) 91.6(2); C(26)−Al(2)−C(25) 95.0(2); P(1)−N(1)−Ti(1) 173.2(3); P(2)−N(2)−Al(1) 133.7(2); P(2)−N(2)−Ti(1) 138.3(2); Al(1)−N(2)−Ti(1) 87.91(16); Ti(1)−C(25)−Al(1) 82.7(2); Ti(1)−C(25)−Al(2) 82.3(2); Al(1)−C(25)−Al(2) 132.9(4); Al(2)−C(26)−Ti(1) 85.0(2); Al(2)−C(26)−Al(3) 102.6(3); Ti(1)−C(26)−Al(3) 167.8(4).

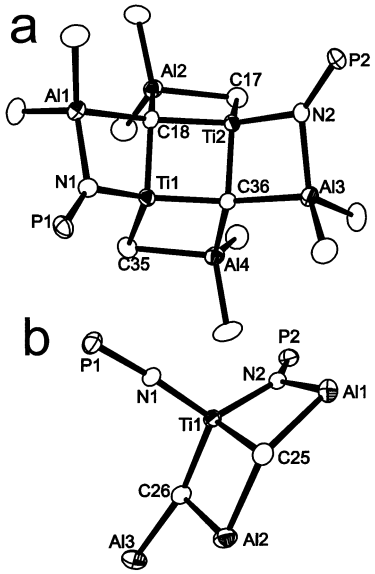

Figure 3. ORTEP drawings of heavy atom cores of (a) **2** and (b) **3**.

(55) Reina, R.; Riba, O.; Rossell, O.; Seco, M.; de Montauzon, D.; Pellinghelli, M. A.; Tiripicchio, A.; Font-Bardia, M.; Solans, X. *J. Chem. Soc., Dalton Trans.* **2000**, 4464−4469.
(56) Reina, R.; Rodriguez, L.; Rossell, O.; Seco, M.; Font-Bardia, M.; Solans, X. *Organometallics* **2001**, *20*, 1575−1579.
(57) Reina, R.; Riba, O.; Rossell, O.; Seco, M.; Gomez-Sal, P.; Martin, A.; de Montauzon, D.; Mari, A. *Organometallics* **1998**, *17*, 4127−4135.

Scheme 1. Reactions and Mechanisms of C−H Activations

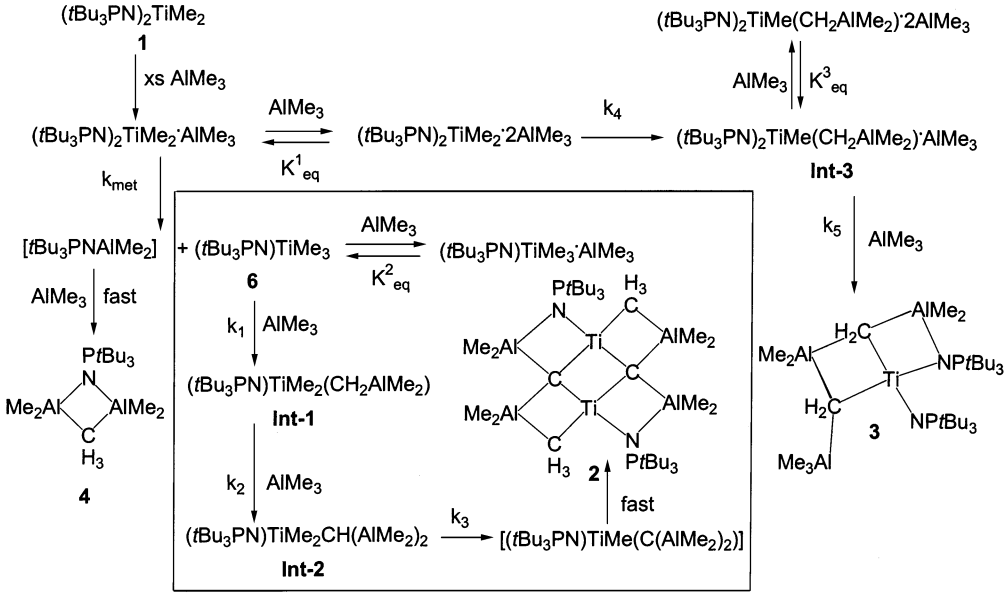

geometries. The Ti1−C35 and Ti2−C17 distances of 2.237(7) Å and 2.223(7) Å are significantly longer than those seen in the four-membered rings of $Cp_2TiCH_2C(Ph)C(Ph)$ (Ti−C 2.11 Å).[58]

A second product, formed in the reaction of **1** with $AlMe_3$, was found to remain in the benzene supernatant decanted from the precipitated **2**. Addition of hexanes precipitated a peach-colored solid **3** in 27% yield. $^{31}P\{^1H\}$ NMR data showed **3** contained two inequivalent phosphinimide resonances at 69.0 and 40.9 ppm, consistent with bridging and terminal phosphinimides, respectively. The ^1H NMR spectrum also revealed doublets at 5.33 and 5.06 ppm and two broad resonances at 3.84 and 1.80 ppm. Each of these signals integrated to one hydrogen and were assigned to two distinct CH_2 groups. Five ^1H resonances near 0 ppm with integral ratios of 3:3:3:9:3 were attributed to four $AlCH_3$ groups and one $AlMe_3$ unit. The $^{13}C\{APT\}$ NMR spectrum confirmed the presence of two phosphinimide ligands, two methylene groups, and the five types of $Al(Me)_x$ groups.

An X-ray structural study of **3** revealed the formulation as $[(t\text{-}Bu_3PN)Ti(\mu^2\text{-}t\text{-}Bu_3PN)(\mu^3\text{-}CH_2)_2(AlMe_2)_2(AlMe_3)]$ (Figure 2). In this species, the Ti coordination sphere is comprised of two phosphinimide ligands and two methylene carbons. One of the phosphinimide ligands is terminal while the other bridges to an $AlMe_2$ fragment, which is also bound to one of the methylene carbons (Figure 3b). The terminal Ti−N bond length of 1.793(4) Å in **3** is similar to that previously reported for **1**, while the bridging Ti−N bond length in **3** of 1.991(4) Å is slightly shorter than that seen in **2** (2.015(5); 2.027(4) Å). The difference in bonding is also reflected in the P−N distances (terminal: 1.597(4) Å; bridging: 1.609(4) Å). The Ti−C distances of 2.013(7) and 2.125(6) Å in **3** are in the range of those reported for the parent **1** (2.121(3) Å, 2.129(3) Å). A second $AlMe_2$ group bridges the two methylene groups while a $AlMe_3$ binds to the second methylene carbon. This geometry gives a pseudo-tetrahedral coordination sphere about Ti. The hydrogen atoms on the two methylene carbons were located and refined. Each of the methylene carbons are nominally five coordinate. The geometry about C(25) is quite distorted with an Al−C(25)−Al angle of 132.9(4)° and Al−C(25)−Ti angles of 82.7(2) and 82.3(2)°. In contrast, the geometry about C(26) is better described as pseudo-trigonal bipyramidal as the Ti−C(26)−Al angle is 167.8(4)° while the Al(2)−C(26)−Ti and Al−C(26)−Al angles are 85.0(2) and 102.6(3)° respectively. A recent neutron diffraction study has confirmed five-coordinate carbon in the species $[Nd(AlMe_4)_3]$.[59]

Monitoring the reaction containing the products **2** and **3** by NMR spectroscopy reveals the formation of a phosphinimide-containing byproduct that gives rise to a resonance at 61.0 ppm. The attribution of this signal to $(Me_2Al)_2(\mu\text{-}CH_3)(\mu\text{-}NP(t\text{-}Bu_3))$ **4** was confirmed by independent synthesis of **4** via reaction of two equivalents of $AlMe_3$ with t-Bu_3PNH at 60 °C. This species is similar to the pyrazolate compounds $(R_2Al)_2(\mu\text{-}N_2C_3R'_2)(\mu\text{-}R)$ recently structurally characterized by Winter et al.[60,61]

Treatment of compound **3** with excess $AlMe_3$ at 25 °C for up to six days showed no reaction. This affirms that there is no reaction pathway by which **3** is transformed to **2**, implying that reaction of **1** with $AlMe_3$ proceeds via competing divergent pathways of C−H bond activation, illustrated in Scheme 1. Although **3** does not react further with $AlMe_3$, it does undergo thermolysis at 60 °C over 26 h to generate a new species **5**. Despite repeated attempts, compound **5** could not be isolated in analytically pure form. Nonetheless, spectroscopic data permitted characterization. The observation of lower field $^{31}P\{^1H\}$ NMR resonances (∼60 ppm) infer the presence of two bridging yet inequivalent phosphinimide ligands in **5**. ^1H and $^{13}C\{APT\}$ NMR data were consistent with the loss of methane from **3** and thus the formulation of **5** as $[Ti(\mu^2\text{-}t\text{-}Bu_3PN)_2(\mu^3\text{-}CH_2)(\mu^3\text{-}CH)(AlMe_2)_3]$.

(58) Tebbe, F. N.; Harlow, R. L. *J. Am. Chem. Soc.* **1980**, *102*, 6151.

(59) Klooster, W. T.; Lu, R. S.; Anwander, R.; Evans, W. J.; Koetzle, T. F.; Bau, R. *Angew. Chem., Int. Ed.* **1998**, *37*, 1268−1270.

(60) Yu, Z.; Wittbrodt, J. M.; Heeg, J. M.; Schlegel, H. B.; Winter, C. H. *J. Am. Chem. Soc.* **2000**, *122*, 9338−9339.

(61) Yu, Z.; Heeg, J. M.; Winter, C. H. *J. Chem. Soc., Chem. Commun.* **2001**, 353−354.

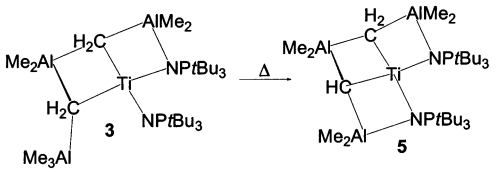

Mechanistic Studies

Monitoring of the reaction of **1** with $AlMe_3$ by $^{31}P\{^1H\}$ NMR spectroscopy revealed a complex series of reactions, generating several intermediate products that grew and were consumed, ultimately giving the products **2**−**4**. On the basis of the $^{31}P\{^1H\}$ NMR chemical shift of 32.5 ppm, one of these intermediates appeared to be (*t*-Bu_3PN)$TiMe_3$ **6**.[53] Thus, to begin to examine this system mechanistically, the simpler reaction of **6** with $AlMe_3$ was studied in detail by $^{31}P\{^1H\}$ NMR spectroscopy. Initially, T_1 measurements were performed on products **2**−**4** to ensure that adequate relaxation delays were employed to permit the correlation of integrals and concentrations. Monitoring the reaction of **6** with varying amounts of $AlMe_3$ (3, 6, 9, 12, 15, 18 equivalents) at 298 K revealed the consumption of the starting material proceeded via an exponential decay with the corresponding generation of **2**. The decay of the concentration of the initial species was found to follow pseudo-first-order decay kinetics when the $AlMe_3$ was in significant excess (Figure 4). In addition, the rate showed a first-order dependence on the concentration of $AlMe_3$. A least-squares fit of the plot of k_{obs} and [$AlMe_3$] (Figure 5) revealed the second-order rate constant k_1 is 3.9(5) × 10^{-4} M^{-1} s^{-1} with an intercept of approximately zero (5(4) × 10^{-5}). These data reveal the initial C−H bond activation of **6** by reaction with $AlMe_3$ proceeds via an overall second-order process. Data for Eyring plots were accessible over a 20 K range (284−304 K). These provide the activation parameters: $\Delta H^{\neq}$ = 63(2) kJ/mol and $\Delta S^{\neq}$ = −80(6) J/mol·K (Figure 6). This negative value of the entropy of activation is consistent with a bimolecular associative process, while the enthalpy value suggests substantial bond breakage in the transition state. The proposed mechanism involves Al−C bond scission forming methane, although attempts to address this point directly via labeling studies are precluded by rapid Al−Me/Ti−Me scrambling that occurs in reaction mixtures of **6** and $AlMe_3$ prior to C−H bond activation. The observed activation parameters compare with those reported for the 1,2 elimination of methane from $(Me_3SiO)_2TiMe(NHSi$*t*-$Bu_3)$ ($\Delta H^{\neq}$ = ∼85 kJ/mol, $\Delta S^{\neq}$ = ∼−48 J/mol).[62] This supports a proposed mechanism in which the orientation of the Al−C and Ti-bound methyl group in a six-membered-ring transition state is a critical feature.

The interaction between $AlMe_3$ and **6** appears to be initiated by Lewis acid−base interactions. Al can interact with the Ti-bound nitrogen atoms or Al-bound methyl groups may interact with the Lewis acidic Ti center (Drawing 2). ^1H NMR spectra show significant broadening of the titanium-methyl resonance upon addition of $AlMe_3$ to **6**, consistent with facile methyl group exchange equilibria. Similarly, bridging methyl interactions between Al and lanthanides have been crystallographically confirmed in a series of species by the research groups of Lappert and subsequently Evans.[63] The observation of both an equilibrium between **6** and **6**·$AlMe_3$ and a second-order C−H bond activation reaction between **6** with $AlMe_3$ suggests that there are both productive and benign modes of interactions between these molecules. Although speculative, it is tempting to suggest that interaction of Al−Me with N−Ti results in a relatively electron deficient Ti center, thus activating the bridging methyl group for C−H activation, prompting the view that interaction with N prompts C−H bond activation, while

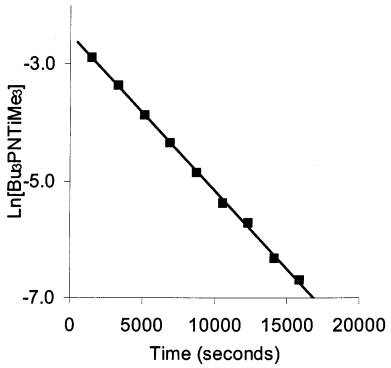

Figure 4. Representative data for the disappearance of **6** vs time at 298 K; $[Ti]_o$ = 0.075 M, $[Al]_o$ = 0.45 M, R^2 = 0.99.

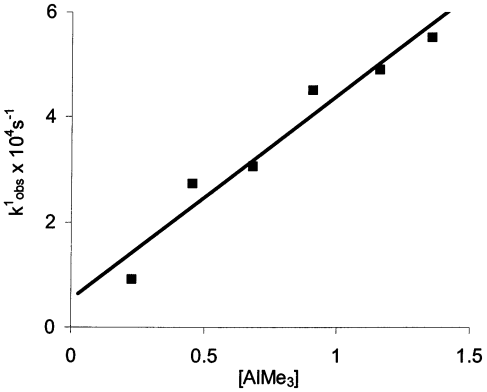

Figure 5. Plot of k_{obs} vs [$AlMe_3$] for the consumption of **6** at 298 K; k_1 = 3.9 × 10^{-4} M^{-1} s^{-1}, $[Ti]_o$ = 0.075 M, R^2 = 0.95.

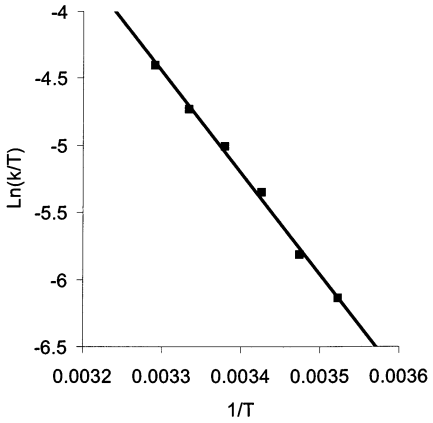

Figure 6. Eyring plot for the disappearance of **6** vs time; $[Ti]_o$ = 0.075 M, $[Al]_o$ = 0.45 M, R^2 = 0.99.

(62) Bennett, J. L.; Wolczanski, P. T. *J. Am. Chem. Soc.* **1997**, *119*, 10696−10719.

(63) (a) Holton, J.; Lappert, M. F.; Ballard, D. G. H.; Pearce, R.; Atwood, J. L.; Hunter, W. E. *J. Chem. Soc., Dalton Trans.* **1979**, 54−61. (b) Holton, J.; Lappert, M. F.; Ballard, D. G. H.; Pearce, R.; Atwood, J. L.; Hunter, W. E. *J. Chem. Soc., Dalton Trans.* **1979**, 45−53. (c) Evans, W. J.; Anwander, R.; Ziller, J. W. *Organometallics* **1995**, *14*, 1107−1109.

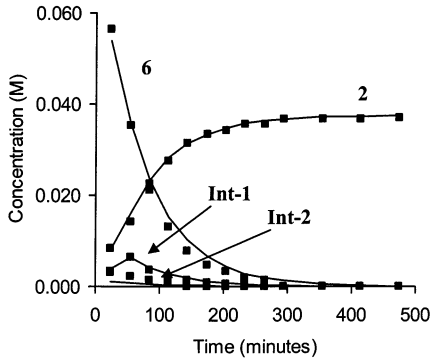

Figure 7. Concentrations vs time plots for the conversion of **6** to **2**. ($[Ti]_o = 0.075$ M, $[Al]_o = 0.90$ M). Observed data are squares and solid lines are calculated values based on Equations 1−4.

methyl bridging/exchange interactions between Ti and Al are benign.

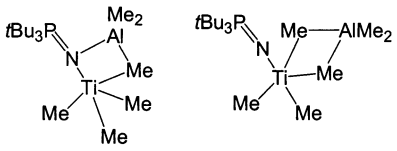

Determination of the mass balance from the integration of the $^{31}P\{^1H\}$ NMR data revealed the presence of two intermediate species that appeared and were consumed during the course of the reaction. These species gave rise to resonances at 38.8 and 39.5 ppm in the $^{31}P\{^1H\}$ NMR spectra and were presumed to be intermediate C−H bond activation products **Int-1** and **Int-2**, respectively. The first of these species to appear (**Int-1**) never exceeded 10% of the initial concentration of the starting material, while the second intermediate species **Int-2** was present in even lower concentrations. The kinetics of the formation and consumption of these intermediates were studied employing data from reactions where 12, 15, and 18 equivalents of $AlMe_3$ were used. These stoichiometries provide adequately slow reaction kinetics so that the concentration profiling of the starting material **2** and the two intermediates could be reasonably measured. At the same time, this stoichiometry provides a minimum of a 10-fold excess of $AlMe_3$ ensuring that the reactions follow pseudo-first-order kinetics. The concentration profiles were calculated employing equations (Equations 1−4) derived from the rate expressions for three sequential reactions. Mass balance provides an expression for the concentration of **2**. In this way, pseudo-first-order kinetic parameters could be obtained for three sequential C−H bond activation reactions. Using k_1 derived above, the solution of these equations gave the rate constants $k_2 = 1.4(2) \times 10^{-3}\ s^{-1}$ and $k_3 = 7(1) \times 10^{-3}\ s^{-1}$. The observed and calculated concentration profiles of the starting material **2** and the two intermediates are in excellent agreement (Figure 7), thus supporting a proposed mechanism involving three sequential C−H bond activations (Scheme 1 inset) in which the initial C−H activation of **6** is rate-determining. Although these observations appear consistent, the inability to acquire "rise-time" data for the low concentration intermediates due to the speed of the reaction may mean the errors on these rate constants are underestimated.

The first C−H activation generating **Int-1** is second-order, dependent on the concentrations of both Ti and Al. A second C−H activation generates **Int-2** containing a Ti bound methine-carbon and two Al atoms. We have previously described the related methine species $Cp^*Ti(\mu^2\text{-}Me)(\mu^2\text{-}NPR_3)(\mu^3\text{-}CH)(AlMe_2)_2$.[50,51] The final C−H bond activation by elimination of methane from **Int-2** would generate a monometallic-carbene species. This compound is not observed during the reaction suggesting it rapidly dimerizes affording the final product **2**. In contrast, sterically demanding and chelating ligands have been shown to stabilize monomeric Ti-carbene species as in the species $[(Me_3SiNPPh_2)_2C]TiCl_2$ recently described by Cavell et al.[64] It is interesting that for **6** the rate of C−H activation increases approximately 5-fold with successive replacement of protons by electron-withdrawing $AlMe_2$ fragments.

$$[\mathbf{6}] = [\mathbf{6}]_o e^{-k1t} \tag{1}$$

$$[\mathbf{int\text{-}1}] = \frac{k_1[\mathbf{6}]_o(e^{-k1t} - e^{-k2t})}{(k_2 - k_1)} \tag{2}$$

$$[\mathbf{int\text{-}2}] = \left[\frac{k_1k_2[\mathbf{6}]_o}{(k_2 - k_1)(k_3 - k_1)}\right]e^{-k1t} + \left[\frac{k_1k_2[\mathbf{6}]_o}{(k_1 - k_2)(k_3 - k_2)}\right]e^{-k2t} + \left[\frac{k_1k_2[\mathbf{6}]_o}{(k_1 - k_3)(k_2 - k_3)}\right]e^{-k3t} \tag{3}$$

$$[\mathbf{2}] = \frac{[\mathbf{6}]_o}{2}\left[1 - \frac{k_2k_3e^{-k1t}}{(k_2 - k_1)(k_3 - k_1)} - \frac{k_1k_2e^{-k2t}}{(k_1 - k_2)(k_3 - k_2)} - \frac{k_1k_2e^{-k3t}}{(k_1 - k_3)(k_2 - k_3)}\right] \tag{4}$$

Returning to the more complex reaction of **1** with $AlMe_3$, reactions employing 5, 10, 15, 20, 25, and 27 equivalents $AlMe_3$ were monitored by $^{31}P\{^1H\}$ NMR spectroscopy at 30 min intervals over 16 h periods (Figure 8). In addition to **2**, resonances attributable to **3** and **4** were observed as well as intermediate species **6** and another intermediate **Int-3**. Resonances in the range 41.0−43.9 ppm and 33.3−31.8 ppm depending on the concentration of $AlMe_3$ were attributed to **Int-3** with the latter resonance also including the signal from **6**. A resonance attributable to **1** is not observed. Rather, the initial species in solution exhibits a single resonance, the $^{31}P\{^1H\}$ NMR chemical shift of which varies with the concentration of $AlMe_3$ over the range 27−32 ppm. The final product ratio of 2:3 varies from 1.3 to 0.5 over the range of concentration of $AlMe_3$ used (Table 2).

The concentration of compound **6** grows in and is ultimately consumed during the reaction. The formation of **6** from **1** is a metathesis affording **4** as the byproduct. The amount of **4** produced in the overall reaction is twice that of **2** in all cases as expected. The rate of formation of **4** was independent of the concentration of $AlMe_3$, and thus the first-order rate constant for the metathesis k_{met} was found to average $6.1(5) \times 10^{-5}\ s^{-1}$ for experiments done with 10, 15, 20, 25, and 27 equivalents of $AlMe_3$. Although the nature of the kinetics of this reaction permitted Eyring plots only over the temperature range 292−

(64) Cavell, R. G.; Babu, R. P. K.; Kasani, A.; McDonald, R. *J. Am. Chem. Soc.* **1999**, *121*, 5805−5806.

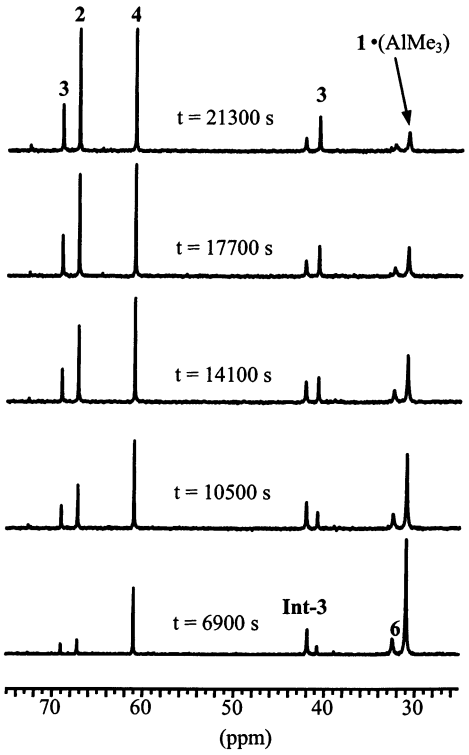

Figure 8. Representative $^{31}P\{^1H\}$ NMR spectra for reaction of **1** with $AlMe_3$ vs time.

Table 2. Observed and Computed Concentration Profiles

	observed concentrations (M)				calculated concentrations (M)[b]			
$[AlMe_3]$	**[2]**[a]	**[3]**[a]	**[4]**[a]	(**[Int-3]** + **[6]**)$_{max}$[c]	**[2]**[a]	**[3]**[a]	**[4]**[a]	(**[Int-3]** + **[6]**)$_{max}$[c]
0.76	0.025	0.023	0.050	0.020	0.025	0.023	0.051	0.018
1.13	0.022	0.028	0.044	0.019	0.023	0.028	0.045	0.018
1.49	0.017	0.033	0.040	0.017	0.018	0.035	0.038	0.018
1.88	0.016	0.032	0.035	0.019	0.017	0.031	0.036	0.020
2.03	0.014	0.034	0.031	0.019	0.017	0.038	0.034	0.020

[a] Concentrations are those observed at 298 K and calculated at reaction completion; $[\mathbf{1}]_0 = 0.075$. [b] Calculated values based on the mechanism were derived employing the program *Chemical Kinetics Simulator*, v1.01[65] using k_1, k_2, k_3, k_{met}, $k_4 = k_{obs}$, and $K^1eq = 0.6(1)$, $K^2eq = 1.5$, $K^3eq = 2$, and $k_5 = 4 \times 10^{-4}$ s^{-1}. [c] Maximum concentration of the two intermediates are listed together as peak overlap precluded accurate determination of the concentration of the individual intermediates.

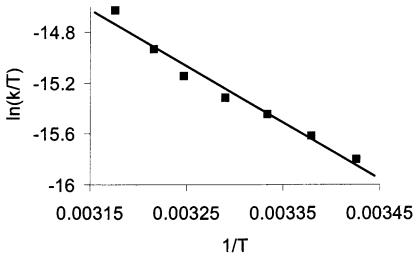

Figure 9. Eyring plot for the appearance of **4** vs time ($[Ti]_o = 0.075$ M, $[Al]_o = 0.750$ M, $R^2 = 0.97$).

315 K, these data provided the activation parameters of $\Delta H^{\neq}_{met} = 37(3)$ kJ/mol and $\Delta S^{\neq}_{met} = -203(9)$ J/mol·K (Figure 9). These data suggest a preequilibrium between **1** and $AlMe_3$ yielding an adduct which undergoes first-order decay to give the products of metathesis. The more negative value of the entropy of activation for metathesis compared to C–H activation of **6** may reflect the relatively large entropy term associated with organization of the adduct required to effect metathesis in

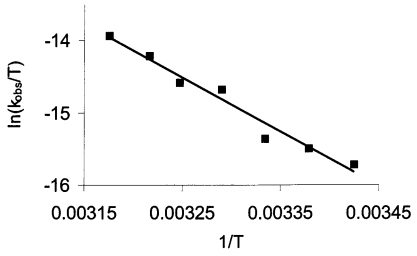

Figure 10. Eyring plot for the appearance of **3** vs time, k_{obs}: overall pseudo-first-order rate constant of formation of **3**, $[Ti]_o = 0.075$ M, $[Al]_o = 0.750$ M, $R^2 = 0.97$.

the more crowded *bis*-phosphinimide complex. The proposition of a preequilibrium between **1** and $AlMe_3$ is also consistent with the observed dependence of the $^{31}P\{^1H\}$ NMR chemical shift for the initial species in solution on the concentration of $AlMe_3$. Such a preequilibrium also accounts for methyl exchange leading to the incorporation of ^{13}C atoms into the TiMe and $AlMe_2$ sites in the products **2** and **3** from ^{13}**1**.

The overall rate constant for the formation of **3** is $k_{obs} = 6(1) \times 10^{-5}$ s^{-1}. The corresponding activation parameters for the formation of **3** were derived from Eyring plots (k_{obs}: pseudo-first-order rate constant) over the temperature range 292–315 K. This showed $\Delta H^{\neq} = 62(5)$ kJ/mol and $\Delta S^{\neq} = -118(17)$ J/mol·K (Figure 10). The enthalpy term is similar to that determined for the activation of **6**, while the entropy term is more negative suggestive of an increased steric barrier to the transition state.

In considering the mechanism of reaction of **1** with $AlMe_3$, one is tempted to postulate competitive divergent reaction pathways involving metathesis and C–H bond activation from a single-starting material. However, such a view is clearly too simple as it does not account for the increased production of **3** with increasing $AlMe_3$. An equilibrium between **1**·$AlMe_3$ and **1**·$(AlMe_3)_2$ (K^1eq, Scheme 1) in which **1**·$AlMe_3$ undergoes metathesis forming **6** en route to **2**, while **1**·$(AlMe_3)_2$ undergoes C–H bond activation ultimately yielding **3**, is consistent with the changing product ratios. As well, as k_{met} is experimentally indistinguishable from k_{obs}, the equilibrium constant is expected to reflect the product/$AlMe_3$ ratios as per Equation 5. For experiments using 10, 15, 20, 25, and 27 equivalents of $AlMe_3$, the product ratios infer $K^1eq = 0.59(5)$.

$$K^1\mathrm{eq} = \frac{[\mathbf{1}\cdot 2\mathrm{AlMe_3}]}{[\mathbf{1}\cdot\mathrm{AlMe_3}][\mathrm{AlMe_3}]} = \frac{[\mathbf{3}]}{2[\mathbf{2}][\mathrm{AlMe_3}]} \qquad (5)$$

In a similar vein, equilibria involving **6** (K^2eq) and **Int-3** (K^3-eq) with $AlMe_3$ must be considered to account for the transient concentrations of **6** and **Int-3**, respectively. Such equilibria are certainly consistent with the anticipated Lewis acid–base interaction between $AlMe_3$ and the phosphinimide complexes and also account for the $^{31}P\{^1H\}$ chemical shift dependence on the $AlMe_3$ concentration. Attempts to experimentally observe such equilibria for **1** and **6** independently by $^{31}P\{^1H\}$ NMR spectra failed as exchange remains rapid even at low temperature (−80 °C).

Further support for the postulate of these equilibria was derived from stochastic kinetic simulations.[65] The concentration

(65) Hinsberg, W.; Houle, F.; Allen, F.; *Chemical Kinetics Simulator*, v1.01; IBM: Almaden Research Center, 1996.

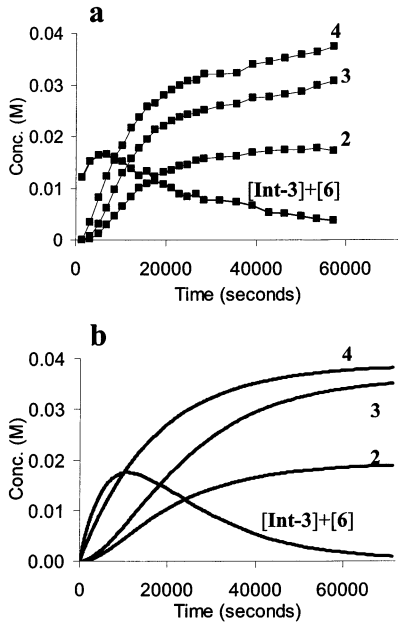

Figure 11. Concentrations vs time plots for the conversion of **1** to **2**−**4** ($[Ti]_o = 0.075$ M, $[Al]_o = 1.49$ M). (a) observed (b) calculated on the basis of stochastic model of mechanism (see Table 2).

profiles of the products **2**−**4**, **6**, and **Int-3** were computed employing the mechanism proposed in Scheme 1. The kinetic parameters, k_1, k_2, k_3, k_{met}, and K^1eq determined above, were employed. It was assumed that the rate-determining step of formation of **3** was a first-order C−H activation (i.e., $k_4 = 6 \times 10^{-5}$ s^{-1}), with the second C−H activation occurring significantly faster although also in a first-order process (i.e., $k_5 = 4 \times 10^{-4}$ s^{-1}). Equilibrium constants (K^2eq, K^3eq) consistent with the observed concentration profiles were determined by an iterative process of computation and comparison to the observed data. Although this approach does not provide a unique mathematical solution for K^2eq, K^3eq, or k_5, the similarity of the computed concentration profiles and those observed experimentally using 10, 15, 20, 25, and 27 equivalents of $AlMe_3$ (Table 2, Figure 11) confirms the role of equilibria in mediating the concentrations of the product and intermediate species. At concentrations of $AlMe_3$ greater than 20 equivalents, unassigned small but discernible transient $^{31}P\{^1H\}$ NMR resonances suggest the possibility of additional equilibria which have not been taken into account.

The reaction of **1** with $AlMe_3$ establishes an equilibrium between **1**·$AlMe_3$ and **1**·$(AlMe_3)_2$. These species follow disparate pathways; the former undergoing metathesis, the latter C−H bond activation. Interestingly, $\Delta G\ddagger$ for these processes are approximately equal and thus competitive. It is reasonable to suggest that a species derived from the interaction between Al−Me and N−Ti would require a significant reorganization to achieve the transition state en route to metathesis. This view is consistent with the high entropy term. Coordination of a second molecule of $AlMe_3$ is expected to yield a more rigid system, incapable of the molecular rearrangement required for metathesis. Instead, C−H activation occurs. The initial activation of a methyl group of **1** occurs about an order of magnitude slower than in **6**. This may reflect increased electron density at Ti in **1**, as reduced Lewis acidity will result in lesser activation of the metal-bound methyl group. In addition, steric crowding may generate a barrier to the C−H bond activation transition state in **1**, thus slowing the reaction relative to **6**. However, once formed, subsequent activation of **Int-3** leads to the formation of the bis-methylene complex **3**. This stands in contrast to the analogous reactions of **6** and Cp′Ti$(NPR_3)Me_2$ where sequential activations occur on a single carbon atom.[50,51] This may be the result of steric crowding, although a process involving proton migration from a methyl group to a methine carbon cannot be excluded.

Conclusions

The reactions of **1** with $AlMe_3$ described herein reveals while the initially competitive reactions of metathesis and C−H activation lead to divergent products, C−H activation results in either case. C−H activation derived from reaction of $AlMe_3$ and an early metal alkyl species has been known since the work of Tebbe on the reagent that bears his name, $Cp_2Ti(\mu\text{-}CH_2)(\mu\text{-}Cl)AlMe_2$.[58] Related multiple C−H activations have also been observed by Roesky et al. in the formation of the Zr and Hf clusters, $[(Cp^*M)_3Al_6Me_8(\mu^3\text{-}CH_2)_2(\mu^4\text{-}CH)_4(\mu^3\text{-}CH)]$.[66,67] While reactions of Ti vapor and methane have been shown by mass spectrometry to give Ti-carbide clusters in the gas phase,[68] previously known synthetic routes to metal-carbide complexes typically involve C−O,[69−71] C−N,[72] or C−C[73] bond cleavage reactions. Thus, the present Ti-phosphinimide derivatives provide rare examples of such competitive pathways which are clean and amenable to detailed study. Moreover, these observations suggest that both ligand metathesis and C−H activation may be competitive deactivation pathways for olefin polymerization catalysts derived from **1** with Al-based activators. In addition, the kinetic data presented here are to our knowledge the first to quantify sequential rates of activation of a methyl group to carbide. The inferred role of the phosphinimide ligand in initiating these reactions suggests that it may be possible to effect intermolecular C−H bond activation with the judicious choice of ancillary ligands and the metal precursor.

Acknowledgment. Financial support from the NOVA Chemicals Corporation and NSERC of Canada is gratefully acknowledged. F.G. is grateful for the award of an NSERC Postdoctoral Fellowship.

Supporting Information Available: Spectroscopic (PDF) and crystallographic (CIF) data. This material is available free of charge via the Internet at http://pubs.acs.org.

JA0260972

(66) Herzog, A.; Roesky, H. W.; Zak, Z.; Noltemeyer, M. *Angew. Chem., Int. Ed. Engl.* **1994**, *33*, 967−968.
(67) Herzog, A.; Roesky, H. W.; Jager, F.; Steiner, A.; Noltemeyer, M. *Organometallics* **1996**, *15*, 909−917.
(68) Wang, L. S.; Wang, X. B.; Cheng, H. *J. Am. Chem. Soc.* **1998**, *120*, 6556−6562.
(69) Caselli, A.; Solari, E.; Scopelliti, R.; Floriani, C. *J. Am. Chem. Soc.* **2000**, *122*, 538−539.
(70) Kolis, J. W.; Holt, E. M.; Drezdzon, M.; Whitmire, K. H.; Shriver, D. F. *J. Am. Chem. Soc.* **1982**, *104*, 6134.
(71) Anson, C. E.; Bailey, P. J.; Conole, G.; Johnson, B. F. G.; Lewis, J.; McPartlin, M.; Powell, H. R. *J. Chem. Soc., Chem. Commun.* **1989**, 442.
(72) Adams, R. D.; Mathur, P.; Segmuller, B. E. *Organometallics* **1983**, *2*, 1258.
(73) Chiang, S. J.; Chi, Y.; Su, P. C.; Peng, S. M.; Lee, G. H. *J. Am. Chem. Soc.* **1994**, *116*, 11181.